TISSUE ENGINEERING: Part A
Volume 19, Numbers 1 and 2, 2013

DOI: 10.1089/ten.tea.2011.0622

In Vivo Transplantation of Autogenous Marrow-Derived Cells Following Rapid Intraoperative Magnetic Separation Based on Hyaluronan to Augment Bone Regeneration

Tonya Caralla, Ph.D.,[1,2] Powrnima Joshi, Ph.D.,[1] Sean Fleury, B.S.,[1] Viviane Luangphakdy, M.S.,[1] Kentaro Shinohara, M.D.,[1] Hui Pan, M.D.,[1] Cynthia Boehm, B.S.,[1] Amit Vasanji, Ph.D.,[3] Theresa E. Hefferan, Ph.D.,[4] Esteban Walker, Ph.D.,[1] Michael Yaszemski, M.D., Ph.D.,[4] Vincent Hascall, Ph.D.,[1] Maciej Zborowski, Ph.D.,[1] and George F. Muschler, M.D.[1]

Introduction: This project was designed to test the hypothesis that rapid intraoperative processing of bone marrow based on hyaluronan (HA) could be used to improve the outcome of local bone regeneration if the concentration and prevalence of marrow-derived connective tissue progenitors (CTPs) could be increased and nonprogenitors depleted before implantation.
Methods: HA was used as a marker for positive selection of marrow-derived CTPs using magnetic separation (MS) to obtain a population of HA-positive cells with an increased CTP prevalence. Mineralized cancellous allograft (MCA) was used as an osteoconductive carrier scaffold for loading of HA-positive cells. The canine femoral multidefect model was used and four cylindrical defects measuring 10 mm in diameter and 15 mm in length were grafted with MCA combined with unprocessed marrow or with MS processed marrow that was enriched in HA^+ CTPs and depleted in red blood cells and nonprogenitors. Outcome was assessed at 4 weeks using quantitative 3D microcomputed tomography (micro-CT) analysis of bone formation and histomorphological assessment.
Results: Histomorphological assessment showed a significant increase in new bone formation and in the vascular sinus area in the MS-processed defects. Robust bone formation was found throughout the defect area in both groups (defects grafted with unprocessed marrow or with MS processed marrow.) Percent bone volume in the defects, as assessed by micro-CT, was greater in defects engrafted with MS processed cells, but the difference was not statistically significant.
Conclusion: Rapid intraoperative MS processing to enrich CTPs based on HA as a surface marker can be used to increase the concentration and prevalence of CTPs. MCA grafts supplemented with heparinized bone marrow or MS processed cells resulted in a robust and advanced stage of bone regeneration at 4 weeks. A greater new bone formation and vascular sinus area was found in defects grafted with MS processed cells. These data suggest that MS processing may be used to enhance the performance of marrow-derived CTPs in clinical bone regeneration procedures. Further assessment in a more stringent bone defect model is proposed.

Introduction

Bone regeneration in large bone defects and complex wounds remains an unsolved clinical challenge.[1] Osteoconductive scaffolds, such as allograft cancellous bone can be successful in small or contained defects. However, success rates drop as defect size increases and in settings compromised by previous scarring, bone loss, and vascular compromise. In more complex settings, surgeons most often utilize autogenous cancellous bone or supplement an osteoconductive scaffold using bone marrow aspirate (BMA) or an osteoinductive agent, such as bone morphogenetic protein-2.[2] BMA contains a heterogeneous population of osteogenic connective tissue progenitors (CTP-Os), which are thought to contribute to new bone formation.[3] However, the prevalence of CTPs is low (1 CTP per 20,000 nucleated cells).[4,5] Moreover, BMA also contains a large number of erythrocytes derived from contaminating peripheral blood, which do not contribute to a bone-healing response. Given the limitation of diffusion of oxygen and other nutrients into a bone grafting

[1]Department of Biomedical Engineering (ND20), Lerner Research Institute, Cleveland Clinic, Cleveland, Ohio.
[2]Department of Biomedical Engineering, Case Western Reserve University, Cleveland, Ohio.
[3]Image IQ, Cleveland, Ohio.
[4]Mayo Clinic, Rochester, Minnesota.

site larger than 1–2 mm in thickness, there is reason to expect that the survival and contribution of CTPs that are transplanted in this environment are compromised by competing nonosteogenic cells.[3] As a result, methods to both increase the number of CTP-Os in a wound site and decrease the number of nonprogenitors are hypothesized to increase the rate or extent of bone formation in a graft site.

Successful bone repair or regeneration in any clinical setting requires CTP-Os. While osteoconductive and osteoinductive materials may improve bone regeneration, only osteogenic cells generate new bone. CTPs are defined as tissue-resident stem or progenitor cells that proliferate to form a colony *in vitro* and can be induced to express one or more connective tissue phenotypes.[3,6] CTP-Os represent the subset of CTPs that are capable of generating osteogenic progeny. Recent data suggest that all or almost all of the new bone formed at the site of a normal fracture is generated by local cells present in the injured tissue site.[7,8] As a result, in settings where the local CTP population is suboptimal, as in most complex defect sites, optimizing the bone-healing response will require transplantation of CTPs. The most available sources of CTPs are autogenous cancellous bone or bone marrow harvested by aspiration. Many preclinical studies demonstrate improved graft performance when marrow-derived cells are added, even to small graft sites in young healthy animals. This strongly supports the premise that the CTP-O population is suboptimal in most clinical settings and that optimal performance from any osteoconductive or osteoinductive material may require augmentation with CTPs.[9–14]

Several markers have been proposed for use in identification and positive selection of osteogenic cells from bone marrow, including STRO-1,[15] CD271,[16] CD49a,[17] CD146,[18] and CD105.[19] We have recently reported that the presence of hyaluronan (HA; also known as hyaluronic acid or hyaluronate) on the surface of freshly isolated marrow-derived cells can also be used as a marker for positive selection.[20]

HA, is a common, but highly regulated component of extracellular matrix. HA is a nonsulfated linear glycosaminoglycan that consists of repeating units of glucuronic acid and N-acetyl-glucosamine. Extracellularly, HA is found as part of the backbone of extracellular matrix structures through proteoglycan binding or attached to the cell surface, forming pericellular coats.[21] Chains of HA are synthesized at the plasma membrane on the cytosolic side and extruded through the cell membrane by a hyaluronan synthase (HAS). Therefore, retention of HA at the cell surface can occur through HAS or through binding to cell HA receptors, notably CD44.

This project was designed to test the hypothesis that rapid intraoperative processing of bone marrow using HA as a marker for positive selection could be used to improve the outcome of local bone regeneration *in vivo*.

Methods

Preparation of allograft

Mineralized cancellous allograft (MCA) bone (canine) was prepared by the Musculoskeletal Transplant Foundation (Edison, NJ) using canine bone from the proximal humerus, proximal tibia, and proximal femur using standardized methods consistent with the guidelines of the American Association of Tissue Banks. Cuboidal chips ($3\times3\times3$ mm) enabled uniform packing of 15–20 chips to fill each femoral defect site.

Collection of heparinized bone marrow

Marrow was aspirated in 2-mL aliquots from 17 sites on the proximal humerus of each coonhound and mixed immediately with 1 mL heparinized saline (1000 IU).

Two sequential buffy coat density separations were done to remove erythrocytes. The heparinized marrow suspension was centrifuged (400 $g\times10$ min) and the buffy coat layer was manually pipetted. The sample was then resuspended in alpha-minimum essential medium (α-MEM) with 20 units of heparin per mL of media and centrifuged again followed by a second manual collection of the buffy coat cells. Buffy-coated marrow (BCM) cells were resuspended in 4–5 mL of separation buffer (Ca^{2+}/Mg^{2+}-free phosphate-buffered saline with 2% fetal bovine serum and 0.5 mM ethylenediaminetetraacetic acid).

Magnetic separation and preparation of MCA implants

BCM cells (range: 0.8- 2×10^9 cells) were labeled with F_C blocker (1 mL, #18553, EasySep™ labeling kit, Stem Cell Technologies [SCT]), and then incubated with biotinylated HA binding protein (HABP) (Calbiochem #385911) (50 μg in 0.5 mg/mL) for 1 h. Excess HABP was removed. An anti-biotin tetrameric antibody complex (1 mL, #18553; SCT) was incubated for 15 min at room temperature followed by magnetic nanobeads (500 μL, #18553; SCT) for 10 min. After increasing the total volume to 30–35 mL using a separation buffer, cells were separated using a custom-built hexapole magnetic system (HMS) for 20 min. Magnetized cells were retained against the channel wall, and the HA^- (non-magnetized) cells were decanted. Two washing steps were performed (10 min/wash). The $HA^-{}_{W1}$ cell fraction was removed after the first wash, and the $HA^-{}_{W2}$ fraction was removed after the second wash. The retained $HA^+{}_{W2}$ fraction was removed from the HMS device, resuspended in a separation buffer, and pelleted for 10 min at 280 g. $HA^+{}_{W2}$ cells were resuspended in 2 mL of autogenous plasma and divided into two 1 mL samples for MCA loading.

Samples of 1 mL of heparinized BMA (hBMA) or 1 mL of magnetically separated $HA^+{}_{W2}$ (MS/$HA^+{}_{W2}$) cells in plasma were loaded onto 0.3 g of MCA by drip soaking. Starting and effluent samples were counted for cells and assayed for CTPs.

Canine femoral multidefect model

Ten skeletally mature purpose-bred female coonhounds (age 2–4, weight 32.1 ± 1.8 kg) were utilized as animal subjects in an Institutional Animal Care and Use Committee (IACUC) approved protocol.[22–24]

The left femur was exposed in an extraperiosteal plane by elevating the vastus lateralis. A customized drill template was fixed longitudinally on the lateral aspect of the femur with two 3.5-mm bicortical screws. Four separate 10-mm diameter and 15-mm long cylindrical defects were then created by sequential use of a circular starting trochar, a pointed drill, and a flat finishing drill. The two cell sourcing methods were assigned to the four available sites in each subject in either an ABBA configuration (five subjects) or a BAAB configuration (five subjects) to control for possible site or

interaction effects related to proximity. Scaffolds loaded with MS/HA^{+}_{W2} cells were denoted as A and scaffolds loaded with hBMA were denoted as B.

The graft sites were protected mechanically using a stainless steel plate that was fixed to the femur using two screws placed into the screw holes created for initial fixation of the drill guide before wound closure.

Animals were allowed free access to food and water and daily exercise. Euthanasia was performed at 4 weeks. Individual defect sites were separated using a band saw and fixed in 10% neutral buffered formalin and transferred at 48 h into 70% ethanol to prevent demineralization. Micro-CT images were obtained of each site before processing for histologic assessment.

Assay for CTPs

Samples from each fraction, BCM, and hBMA were counted in a Beckman Coulter ViCell XR Cell Counter (Beckman Coulter, #731050). Cells were plated at a density of 250,000 cells/chamber (4.2 cm^2), and cultured at 37°C at 5% CO_2 with medium changes on days 2 and 3. The osteogenic medium consisted of α-MEM with 10% fetal bovine serum, 1 unit/mL penicillin, 0.1 mg/mL streptomycin, 10^{-8} M dexamethasone, and 50 μg/mL ascorbate. Day 6 cultures were fixed with 1:1 acetone:methanol for 10 min and stained for nuclei (DAPI) and osteoblastic activity (alkaline phosphatase [AP]).[25] Chambers were scanned and analyzed using Colonyze™ software, identifying colonies containing eight or more cells in a cluster.[25,26] CTP prevalence, defined as the number of CTPs/10^6 cells plated, was obtained. The number of cells/colony and AP area/cell number was quantified for each colony. Phase-contrast microscopy was used to illustrate cell morphology using a Leica DMI 4000B scope with a Q Imaging Retiga 2000R camera.

Microcomputed tomography acquisition and analysis

Quantitative assessment of each graft site was done using microcomputed tomography (micro-CT) and 3D segmental image postprocessing using an eXplore Locus micro-CT scanner (GE Healthcare) at 45-μm resolution.

Bone formation within the defect site was identified based on electron density at or above the density of native trabecular bone (1000 ± 100 HU) by a blinded operator. A defect template, 10 mm in diameter and 15 mm in length was manually positioned. Voxels within the defect above the threshold mineral density were segmented as bone. Percent bone volume (%BV) was measured by counting the fraction of bone pixels within the defect. The pattern and density of bone formation in each defect was plotted for visualization by projecting %BV data as a 2D contour plot using a gray scale range of 0%–30% BV, where the X-axis indicates radial position from the center of the defect to the edge (range 0–5 mm) and the Y-axis represents vertical position within the defect from the bottom to the opening at the lateral cortex (range 0–15 mm). BV data were subdivided into regions of interest based on differences in local tissue environment. The pericortical (PC) region (between 8 to 12 mm from the bottom of the grafted site) represents the region of the graft site that is adjacent to the cortex, where the contribution of cells from periosteum, cortex, and endosteum may contribute to new bone formation. In contrast, the intramedullary (IM) region (between 3 to 7 mm from the bottom of the grafted site) is separated from the endosteal sources of osteogenic cells and bounded only by cells from the marrow cavity. The PC and IM regions are further divided into center, middle, and outer regions based on the radial position within the defect site. The scaffold performance in the central region of the defect was projected to be the most discriminating with respect to likely efficacy in larger defects (Fig. 1).

To minimize the confounding effects of variation in %BV that would be unrelated to the scaffold performance, the region of interest for analysis of data within the defect was carefully defined. Variation due to nonradially oriented boundary effects at the top soft tissue interface and the bottom endocortical interface was minimized by eliminating the top and bottom 3 mm of each defect from analysis. The very center (0–0.25 mm) was removed from analysis due to the high variability created in data near the center. Finally, data from the very edge of each defect (4.75–5.0 mm) was also removed to minimize the potential for random inclusion of existing cortex in the analysis due to any small error in positioning of the defect template.

Histological analysis

Histology was performed at the Bone Histomorphometry Laboratory at Mayo Clinic. Each specimen was dehydrated in a graded series of alcohols, and embedded in polymethylmethacrylate without decalcification. Specimens were sectioned (5 μm) along the vertical axis in the middle of the defect site and stained with modified Goldner's Trichrome and a hematoxylin and eosin stain. Sections were scanned using a NanoZoomer Digital Pathology System (Hamamatsu) and analyzed using the software package IHC score (Bacus Laboratories, Inc.).

The PC and IM areas were analyzed across the entire defect width at 10 and 5 mm, respectively, from the bottom of the defect. The center, middle, and outer regions were compared used the same radial dimensions as in micro-CT analysis. Quantitative evaluation was performed with specific assessment of the area of new bone formation, woven bone, vascular sinus spaces, fibrous marrow, hematopoietic bone marrow, and residual allograft material.

Statistical analysis

Due to the baseline variation between subjects in CTP prevalence, the prevalence for each sample was normalized to the BCM. These standardized values were log base 2 transformed to obtain a Gaussian distribution, and the means and 95% confidence intervals were calculated. Back transformation was used to provide the geometric mean and the 95% confidence interval, providing the relative magnitude of change from the BCM. An ANOVA with the *post hoc* Tukey's test was used for comparison of fractions between different process steps.

For micro-CT data, a mixed model ANOVA was used to test for significant differences between scaffolds (hBMA or MS/HA^{+}_{W2}), sites (proximal or distal), depth regions (PC or IM), and radial distance (center, middle, or outer). The effect of dog was accounted for as a random factor. All interactions were included. The analysis was performed with JMP 9.0 (SAS®; Cary).

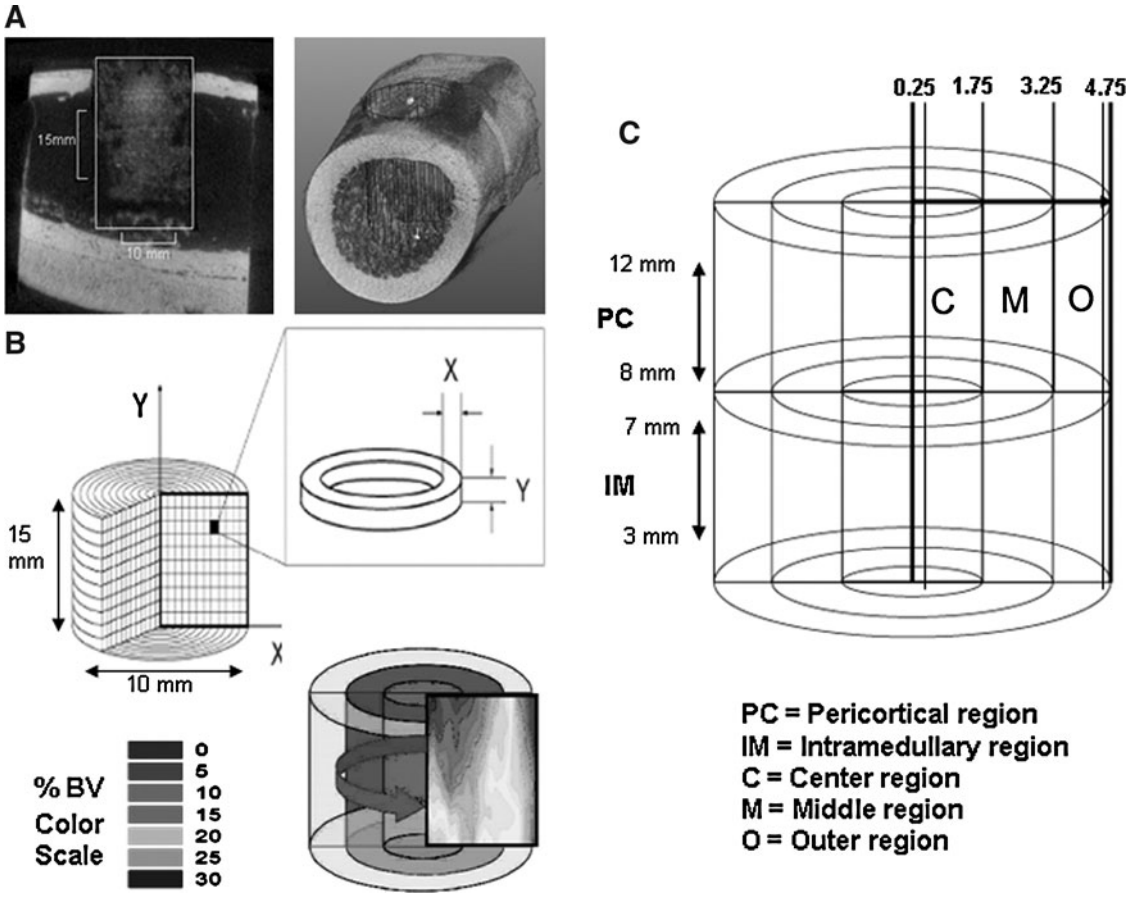

FIG. 1. Micro-CT processing technique. **(A)** The 3D defect volume is defined using a standard 10-mm diameter × 15-mm long cylinder. **(B)** Following segmentation, bone volume (BV) data are mapped onto a color 2D contour plot using a scale from 0% to 30% BV. **(C)** The defect site is divided into regions for analysis. The pericortical (PC) region and the intramedullary (IM) region are defined based on vertical position from the bottom of the defect. Three regions of depth are defined based on radial distance from the center in millimeters: Center (C) = 0.25–1.75 mm, middle (M) = 1.75–3.25 mm, and Outer (O) = 3.25–4.75 mm.

Results

Comparison of hBMA and BCM following density separation

The mean concentration of cells in the hBMA sample increased from 61.5×10^6 cells/mL to 123.6×10^6 cells/mL, with a mean cell yield of 42.3% ± 8.6%. The mean prevalence of CTPs in the hBMA and BCM samples were not different (93.6 ± 61.1 CTPs/10^6 cells vs. 89.5 ± 55.3 CTPs/10^6 cells, respectively), while the mean concentration of CTPs in the hBMA increased from 5500 ± 3600 CTPs/mL to 11,800 ± 9200 CTPs/mL, with a CTP yield of 53.4% ± 40.7%.

Comparison of the MS fractions

The majority of cells partitioned to the HA^- fraction (67.5% ± 10.2%). The HA^-_{W1} sample contained fewer cells than the HA^- fraction (14.7% ± 4.3%, $p < 0.0001$), and more cells than the HA^-_{W2} fraction (5.2% ± 2.5%, $p = 0.0045$). Only 7.8% ± 2.7% of the starting cell population was retained as HA^+_{W2} cells ($p < 0.0001$ compared to HA^-)

CTP prevalence (P_{CTP}) varied significantly between the different MS fractions as illustrated in Figure 2. Each fraction is standardized to the P_{CTP} of the BCM (line at 1). HA^+_{W2} P_{CTP} was 2.0-fold greater than the BCM sample (95% CI 1.2, 3.1), indicating enrichment of CTPs.

HA^- P_{CTP} was 9.8-fold lower than the BCM (95% CI 0.0021, 0.21). HA^-_{W1} P_{CTP} was 3.7-fold lower than the BCM (95% CI 0.082, 0.49).

A large difference was found when comparing P_{CTP} in the HA^- population and the HA^+_{W2} population. The ratio of P_{CTP} in the HA^+_{W2}/HA^- population was 18.3-fold ($p = 0.0001$), indicating that the first separation was most effective in removing non-CTPs without displacing CTPs. The first separation resulted in the removal of 67.5% of all nucleated cells and only 8.5% of the CTPs. The first washing step (HA^-_{W1}) resulted in the removal of 14.7% of the nucleated cells and only 4.7% of the CTPs, and the second washing step (HA^-_{W2}) resulted in the removal of 5.2% of the nucleated cells and 6.6% of all of the CTPs.

Comparison of colony metrics

The number of cells per colony was similar in all fractions (Supplementary Fig. S1; Supplementary Data are available online at www.liebertpub.com/tea). The area of AP staining

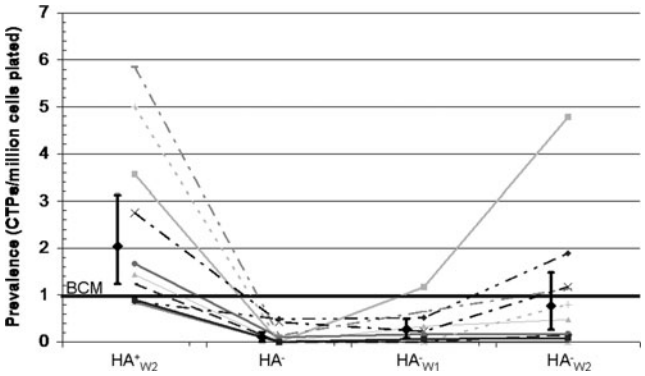

FIG. 2. Connective tissue progenitor (CTP) prevalence of each fraction after magnetic separation (MS) processing, standardized to the buffy-coated marrow (BCM). Geometric means (diamonds) and 95% confidence intervals are presented along with data from each subject (lines).

per cell was similar in the colonies formed from all fractions, with the exception of the HA^-_{W1} samples, where the AP area per cell standardized to the BCM sample was 0.54-fold (CI 0.26, 0.87) (Supplementary Fig. S2). Supplementary Figure S3 illustrated the morphology of cells within colonies for the hBMA, HA^+_{W2} and HA^- fractions.

Accounting for CTPs after MS

The cell yield after MS was 95.1%±11.2%. The total number of CTPs in each fraction can be calculated based on the product of the total number of nucleated cells in a given sample x (N_x) and the $P_{CTP\text{-}O}$ in sample x. While a mean of only 4.9% of cells was lost, a mean of 58.3% of CTPs was not found among the four MS fractions. The HA^+_{W2} fraction only contained 7.8% of the nucleated cells, but 21.9%±17.3% of the CTPs, consistent with the increase in P_{CTP}. However, the HA^-, HA^-_{W1}, and HA^-_{W2} contained only 8.5%±14.3%, 4.7%±5.7%, and 6.6%±12.1% of all CTPs, respectively. Since the BCM sample contained 53.4% of all of the CTPs that were present in the initial hBMA sample, this suggests a loss of 82.9%±13.5% of all CTPs during the cell preprocessing and MS processing.

Allograft loading

The mean number of cells in the starting sample that was loaded onto allograft for the MS/HA^+_{W2} sample was 36.6±13 million cells and for the hBMA sample was 61.5±7.2 million cells. The retention efficiency for cells (RE_{Cells}) loaded onto the MCA matrix was calculated as cells retained/cells loaded.[10,11] RE_{Cells} for the MS/HA^+_{W2} population was 41.8%±18.4%, and RE_{Cells} for the hBMA population was 32.8%±11.6% (not different). However, the retention efficiency for CTPs (RE_{CTPs}) was significantly higher in the MS/HA^+_{W2} samples (75.7%±22.2% vs. 49.0%±20.4%) ($p=0.012$).

The selection ratio (SR) (% of CTPs/% cells retained) in the MCA graft was 2.1±0.9 for MS/HA^+_{W2} samples, and 1.6±0.7 in the hBMA samples, which was not significantly different. After loading hBMA, the CTP prevelance was 1 CTP for every 14,900 nucleated cells in the graft. After loading MS/HA^+_{W2}, there was 1 CTP for every 3600 nucleated cells in the graft ($p=0.0283$). The mean number of cells retained in the graft was 16.1±10.4 million cells for MS/HA^+_{W2} and 20.5±8.7 million cells for hBMA. The mean number of CTPs retained in the graft was 5800±4100 for MS/HA^+_{W2} and 3300±3100 for hBMA. In MS/HA^+_{W2} grafts, the number of CTPs retained was higher and the number of nucleated cells was lower.

In vivo *implantation in the canine femoral multidefect model*

There were no surgical or postoperative complications.

Two-dimensional contour plots of mean %BV across all 10 subjects are presented in Figure 3 illustrating the pattern, distribution, and density of bone formation for all scaffolds. The highest %BV was found at the periphery of the defect, with variable levels of penetration into the middle and central regions. In addition, in all cases, %BV was highest in the PC region of the defect, and lower in the IM region.

In Figure 3, the %BV for each group is presented as a 2D plot that illustrates the change in %BV relative to depth within the defect. Data for the PC and IM regions are presented separately. Both MS/HA^+_{W2} and hBMA loaded grafts showed robust bone formation at 4 weeks.

While the defects grafted with MS/HA^+_{W2} cells had a slightly higher %BV than sites grafted with hBMA, the difference was not statistically significant as assessed by micro-CT. Excluding the residual allograft, the mean %BV for the overall defect for the MS/HA^+_{W2} group was 33.1% (95% CI 29.1, 37.1), and mean %BV for the hBMA group was 30.7% (95% CI 26.7, 34.7). The mean %BV in the PC region (36.2% standard error (SE): 2.1%) was significantly greater than the IM region (27.7% SE: 2.1%) ($p<0.0001$).

Histological analysis

Histological analysis showed an advanced stage of bone formation, remodeling, and marrow reconstitution in both groups. Active bone remodeling with formation and resorption occurred on both residual allograft and new bone surfaces. New bone was synthesized on the surface of the allograft throughout the defect. Marrow space remodeling with vascular spaces and patches of hematopoietic marrow were seen in both groups. Figures 4 and 5 illustrate representative images.

Figure 6 provides histomorphometric data of bone and soft tissue composition in defects grafted with MS/HA^+_{W2} or hBMA loaded MCA. The percent of new bone formed was significantly higher in the MS/HA^+_{W2} defect sites ($p=0.039$). Residual allograft was present in both groups with a trend toward less residual allograft in the MS/HA^+_{W2} group (not significant). There was significantly more sinus area in the MS/HA^+_{W2} group compared to the hBMA group ($p=0.024$), indicating an increase in vascularity in the MS/HA^+_{W2} defect sites. There was a trend toward reduced fibrous tissue in the MS/HA^+_{W2} group, but this was not statistically significant.

Figure 7 illustrates the histomorphological analysis in the PC and IM regions. The IM region exhibited a higher fraction of hematopoietic marrow and vascular sinusoids and less fibrous tissue than the PC region in both groups. There was increased new bone area and woven bone in the PC region, consistent with micro-CT data.

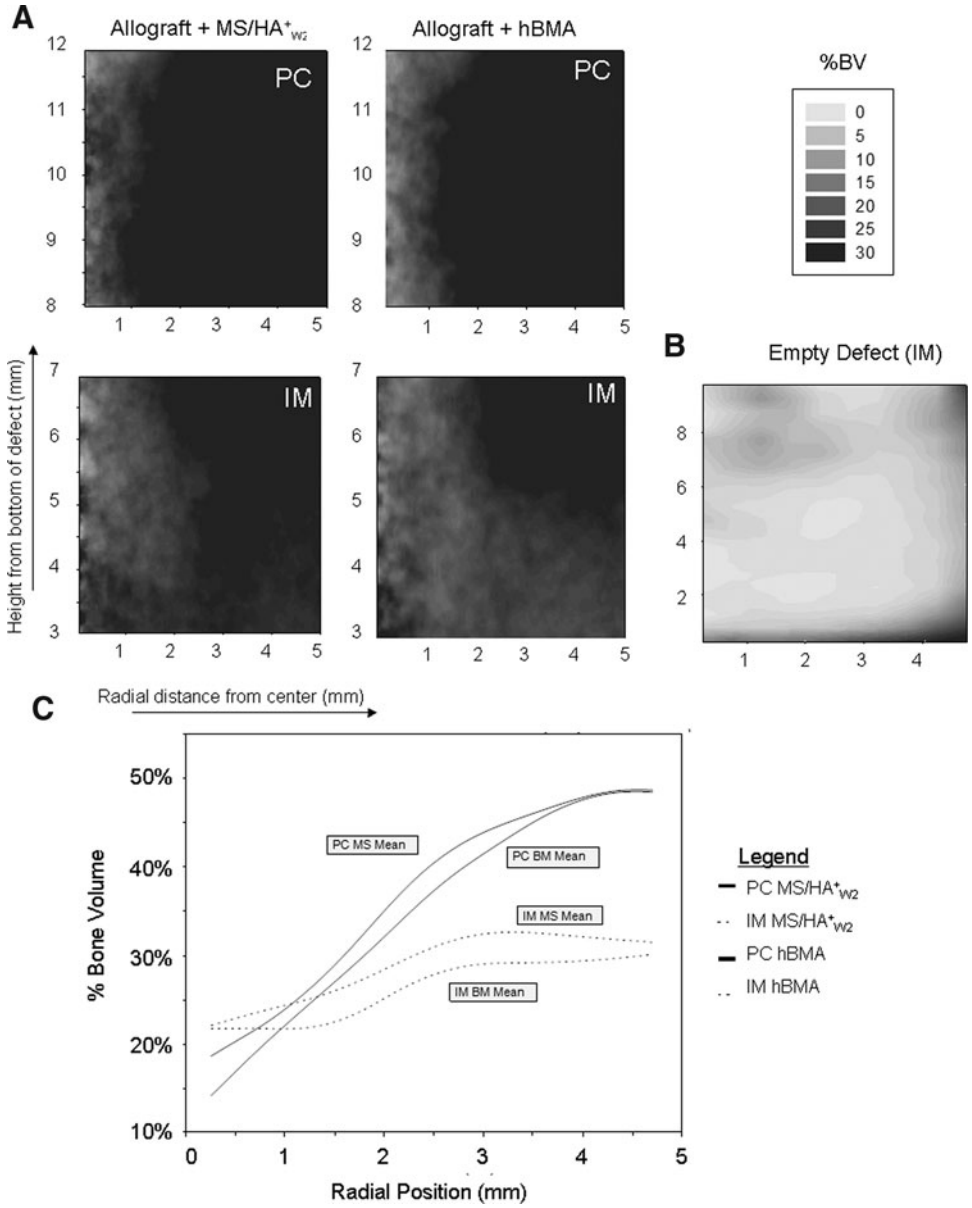

FIG. 3. Results of microcomputed tomography. **(A)** Two-dimensional contour plots of mean percent bone volume (%BV) separated into PC and IM regions showing 0%–30% BV. **(B)** Historical data showing the empty defect in the canine femoral multidefect (CFMD) at 4 weeks in the IM region (2–9 mm from the bottom of the defect). **(C)** 2D plot illustrating %BV as a function of radial position. PC and IM regions are plotted for heparinized bone marrow aspirate (hBMA) and MS/HA^{+}_{W2} defect sites

Discussion

These data support the hypothesis that rapid intraoperative processing of bone marrow using HA as a marker for positive selection can improve the outcome of local bone regeneration *in vivo*. Histomorphometric assessment, enabling the effect of residual unresorbed allograft to be excluded from the estimate of total BV, demonstrated that the volume of new bone formation was significantly greater when MS was used. The area of vascular sinusoids was also significantly greater compared to hBMA. These findings suggest that MS may be a useful clinical method for enhancing the performance of marrow-derived cells.

The MS processing strategy used here is designed to address the profound challenge of cell survival following transplantation into defects greater than 1–2-mm thick, where the imbalance between diffusion of oxygen and the metabolic demand of cells allow few cells to survive in deeper regions of the graft.[3] A logical strategy for improving bone regeneration is to increase the concentration of bone forming cells. However, in larger defects, survival of these cells may be limited unless methods are also designed to limit (deplete) the number of nonprogenitors (i.e., cells that do not contribute to new bone formation) and/or cells that may impair or inhibit the survival and differentiation of CTPs, either by the release of inflammatory or proapoptotic cytokines or in death contributing to secondary inflammation (and associated metabolic demand).

MS processing used here to isolate cells in the MS/HA^{+}_{W2} was successful in both increasing the concentration of CTP-Os among transplanted cells and in depleting nonprogenitors and red blood cells. This finding was consistent with the finding in a previous study.[20]

The outcome of MS processing of canine marrow in the current study was consistent with our previous experience with human marrow, with one exception. When initially

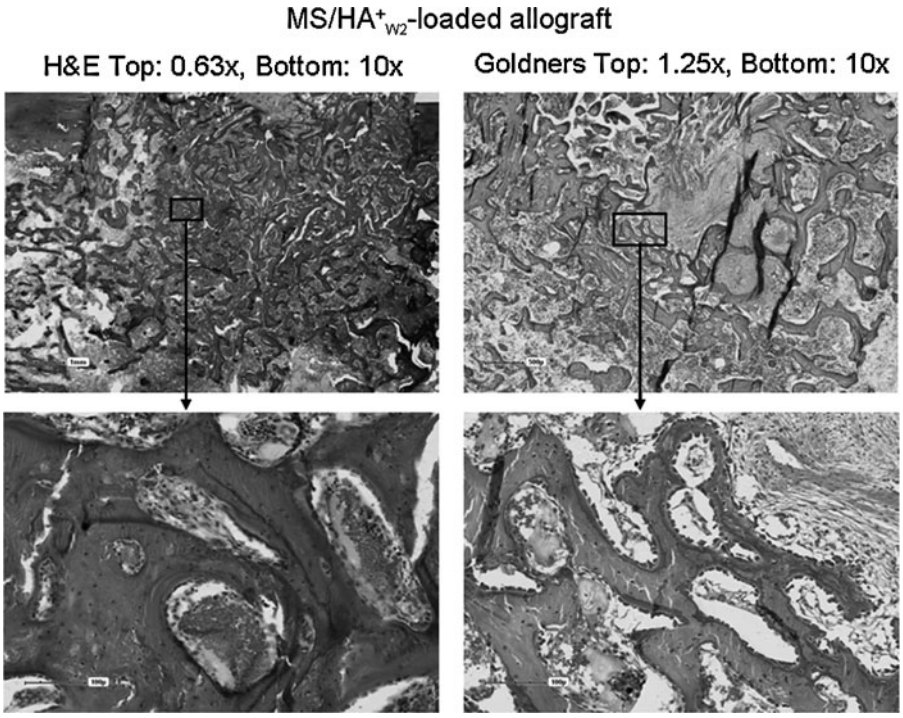

FIG. 4. Histological staining of site grafted with allograft loaded with magnetically separated hyaluronan (HA)-positive cells ($MS/HA^{+}{}_{W2}$ group).

reported in human marrow, we found that the HA^{+++} population had a 3.4-fold higher prevalence than BCM, but also that the colonies formed by HA^{+++} hCTPs were more proliferative and exhibited increased AP staining than the BCM.[20] In the current study using canine marrow, the cCTPs that were present in the $MS/HA^{+}{}_{W2}$ fraction demonstrated a 2.0-fold greater prevalence, but there was no difference in proliferation (cells per colony) nor in AP staining between colonies formed by cCTPs in the $MS/HA^{+}{}_{W2}$ fraction when compared to colonies formed by cCTPs in the BCM or in other fractions. It is not clear if the difference in this finding represents a difference in biology of marrow-derived CTPs between humans and canines, or if these findings represent differences in processing protocols. The processing methods used in the previous work in humans involved three separate steps of magnetic separation (MS) to provide an HA-, HA^{+}, and HA^{+++} population using a much smaller volume of material and a smaller magnet. In contrast, MS

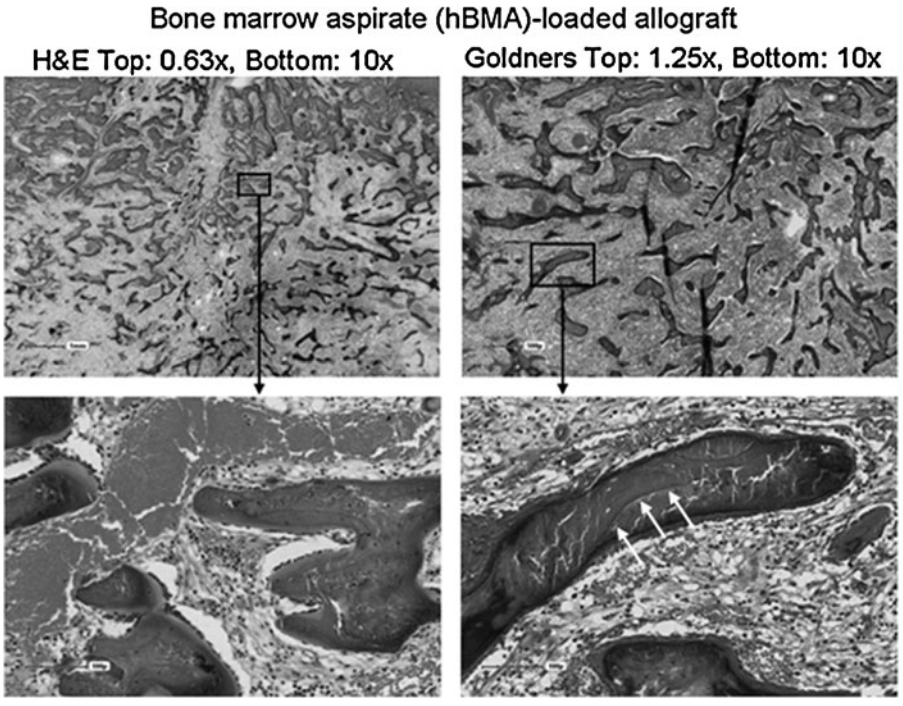

FIG. 5. Histological staining of site grafted with allograft loaded with hBMA group. Three white arrows denote the boundary between unresorbed allograft and newly formed mineralized bone. Residual allograft can be distinguished from newly formed bone due to the lack of osteocytes in the lacunae of the residual allograft.

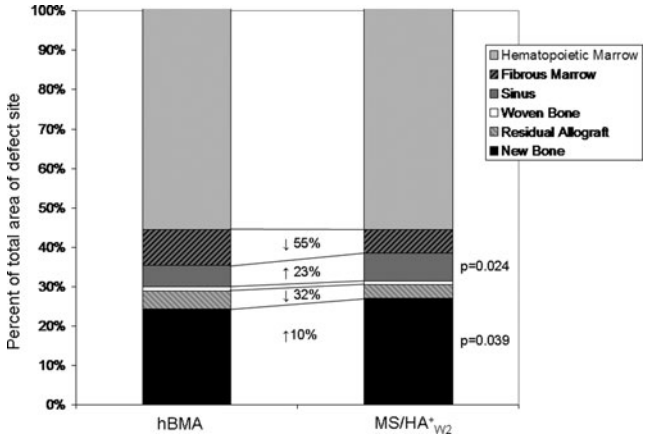

FIG. 6. Histomorphological analysis of bone and soft tissue composition in defects grafted with MS/HA^{+}_{W2} or hBMA loaded mineralized cancellous allograft (MCA). The change in the percent of the total defect area from hBMA sites to MS/HA^{+}_{W2} sites is shown with arrows indicating an increase or decrease in area. Significantly higher new bone area and higher vascular sinus area were found in defects grafted with MS/HA^{+}_{W2} cells.

processing here involved only a single step of MS followed by two washing steps to provide a HA^{+}_{W2} population. The labeling protocol was similar in both cases as were the field strength of the magnets used for separation (0.64 tesla for the EasySep system used in human marrow, and 0.74 tesla for the HMS magnet used here). Further work will be needed to distinguish between species-specific and process-specific differences.

Despite the positive *in vivo* effect of MS processing, an analysis and accounting of the fate of cells and CTP-Os during the processing suggests that there is significant room for process improvement. The first step in the separation,

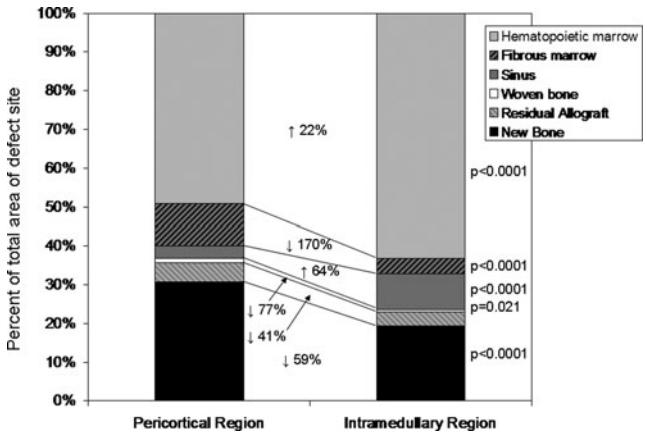

FIG. 7. Histomorphological analysis of bone and soft tissue composition in the PC and IM regions. The change in the percent of the total defect area from PC to IM regions is shown with arrows indicating an increase or decrease in area. The IM region exhibited a higher fraction of hematopoietic marrow and vascular sinusoids and less fibrous tissue than the PC region. There was increased new bone area and woven bone in the PC region.

capture of HA^{+} cells and decanting of HA^{-} cells that were not retained, was the most effective step, resulting in the depletion of 67.5% of all of the nucleated cells with a loss of only 8.5% of the CTPs. The first washing step (HA^{-}_{W1}) resulted in the removal of 14.7% of all of the nucleated cells and only 4.7% of the CTPs. This fraction had a significantly lower CTP-O prevalence than the BCM, suggesting that this step is also effective at removing more nucleated non-progenitor cells than CTPs. However, in the second wash step, the CTP prevalence in the HA^{-}_{W2} fraction was not significantly different than BCM, indicating that the concentration of CTPs removed in the second wash was higher than that removed in the first separation or the first wash step. Elimination of this second wash step would have preserved an additional 6.6% of CTPs.

In addition to opportunities to improve efficiency in the MS processing steps, there is also room for improvement in steps previous to MS during buffy coat preprocessing. Approximately, 45% of all CTPs in the initial sample were lost during the process of preparing the BCM sample. These CTPs may have been lost due to adherence of CTPs to the surface of the containers used during preparation. In addition, many CTPs may have a cell density that is not low enough to allow separation into a buffy coat layer, and are retained in the red cell fraction during density separation. Alternative methods for preparation of the starting sample to remove RBCs, while preserving CTPs, need to be explored.

Sodium heparin was used as an anticoagulant in the preparation of both the MS/HA^{+}_{W2} samples and the hBMA samples. Therefore, a small amount of heparin may have bound to the surface of cells and allograft in both groups. In the case of MS/HA^{+}_{W2} sample, heparin was removed after buffy coat isolation when the sample was resuspended in the MS buffer. The hBMA sample was loaded in the original aspiration suspension. We do not expect heparin to have played any bioactive role in the outcome of this experiment. In previous unpublished work we have compared the *in vitro* performance of CTPs harvested by aspiration using either heparin or EDTA and found no significant difference in colony-forming efficiency. Similarly, we are not aware of any studies that have suggested that the performance of allograft matrix is modulated by exposure to small quantities of heparin.

It should be noted, however, that in some settings prolonged or repeated exposure to heparin can retard bone regeneration. For example, daily subcutaneous injection of heparin in rats resulted in a dose-dependent reduction of bone density and volume.[27,28] In a rabbit femoral condyle defect model, a 6-week course of twice daily subcutaneous injection was associated with a reduction of new bone formation.[29] However, another similar study in a rabbit femoral condyle model showed no significant difference in bone regeneration using daily heparin injection (also for 6 weeks).[30] In our study, however, exposure to heparin occurs only at the time of bone marrow harvest and implantation, and the amount of heparin remaining in the scaffold at the time of implantation is low and should rapidly diffuse out of the implant site. The cells within the allograft implant are not exposed to any additional heparin after implantation and throughout the 4-week time frame before euthanasia.

The fact that CTPs retain their ability to adhere to MCA following MS processing is an important finding. This

finding allows cell populations that are processed using MS methods to be combined with scaffold materials and transplanted into a graft site. Adherence to the surface of a biomaterial greatly increases the likelihood that the transplanted cells will be retained at the site and enables manipulation and placement of the processed cells into a defect. The high retention efficiency during loading indicates that MS processing did not compromise CTP adherence properties. Moreover, the SR greater than 1.0 also indicates that CTPs were preferentially retained on the allograft chips using simple drip soaking loading methods (i.e., CTPs were more likely to be retained than non-CTPs), providing an additional step in which nonprogenitors can be further depleted before implantation.

The canine femoral multidefect (CFMD) model used here has proven to be an effective system for rigorous and relatively rapid objective comparison between bone grafting materials and strategies in the setting of a modestly large defect in a large animal. The value of directly comparing two grafting techniques in single animal controls for variation between subjects and increases statistical power by offering paired comparisons, which in turn reduce the number of subjects needed to address a given comparison.[22–24] Defect sites and performance are reproducible. Very importantly, the defects are large enough so that the center of the defect will become profoundly hypoxic within 2–3 days following surgery. As a result, it would be expected to be sensitive to changes in cell transplantation strategies that might limit hypoxia and improve the survival of transplanted cells. Previous experience has demonstrated that the canine proximal humerus is a reliable source of hematopoietic bone marrow containing osteoblastic progenitors, with yields of nucleated cells and CTPs that are comparable to human iliac crest aspirates.[31]

The CFMD model proved to be a limitation in this study in one respect. Bone regeneration in the MCA supplemented with hBMA was so robust compared to many previous scaffolds that it left relatively little room for improvement. This resulted in a potential ceiling effect in which the magnitude of effect from modification of the cellular environment within MCA might be underestimated. Even though a positive effect was found, this finding suggests that if the benefits of MS processing of marrow is to be confirmed and the value of making further improvement in cell yield and selection is to be tested, this assessment should be performed in an even more stringent model involving a larger defect, and perhaps, a soft tissue environment compromised with respect to scarring and tissue loss, and therefore more representative of the most challenging clinical defects. Further assessment using other less robust scaffolds as substrates may be considered, recognizing this potential limitation.

The material properties of the bone that is regenerated in response to various strategies or materials will have important clinical implications. However, the CFMD model has been designed primarily as a tool for rapid screening and objective comparison between graft materials based on bone formation and histology or histomorphometry. The distribution of the defects does not lend themselves well to isolation of individual sites for testing of mechanical properties that are clinically relevant to bone regeneration in long bones (e.g., stiffness, strength in the setting of bending, and torque loads).

The intention of this work is to use the CFMD model to identify optimal materials and cell strategies, and then to advance those that perform best on metrics of bone formation into more rigorous segmental defect models. In these segmental defect models, where one and only one method is assessed in a given limb, mechanical testing will likely become a valuable adjuvant to assessment, particularly in comparing materials and strategies that generate comparable amounts of mineralized tissue based on CT analysis.[23]

In summary, this work tested a novel approach to enriching CTPs from a fresh BMA that has not been previously evaluated as a therapeutic strategy. In a previous manuscript, we reported the initial observation that HA could be used as a marker to enrich CTPs using MS processing based on *in vitro* colony formation using small-scale processing.[20] This article demonstrates both that MS processing using HA as a marker for selection can be scaled up to allow processing of clinically relevant numbers of cells in a new MS system and the first *in vivo* proof of concept that selection based on HA provides an enriched cell source that increases the rate and extent of bone formation in a large animal model. These data demonstrate that rapid intraoperative processing using HA for positive selection of marrow-derived progenitors represents a potential therapeutic strategy for cell sourcing for application in bone tissue engineering. Further optimization and comparison to alternative clinically relevant cell sourcing options is necessary using the CFMD model and more rigorous clinically relevant models.

Acknowledgments

We would like to acknowledge Rick Rozic for micro-CT and Colonyze imaging, Tess Henderson for micro-CT analysis, Jason Bryan for Colonyze development, James Herrick for histological staining and analysis, and the Musculoskeletal Transplant Foundation for providing allograft. This research was sponsored by the Armed Forces Institute of Regenerative Medicine award number W81XWH-08-2-0034. The U.S. Army Medical Research Acquisition Activity, 820 Chandler Street, Fort Detrick MD 21702-5014 is the awarding and administering acquisition office. The content of the manuscript does not necessarily reflect the position or the policy of the Government, and no official endorsement should be inferred.

Disclosure Statement

No competing financial interests exist.

References

1. Bishop, G.B., and Einhorn, T.A. Current and future clinical applications of bone morphogenic proteins in orthopaedic trauma surgery. Int Orthop **31,** 721, 2007.
2. Bucholz, R., Heckman, J., and Court-Brown, C. (Eds.). Rockwood and Green's Fractures in Adults, 6th edition. Philadelphia, PA: Lippincott, Williams, & Wilkins 2006.
3. Muschler, G., Nakamoto, C., and Griffith, L. Engineering principles of clinical cell-based tissue engineering. J Bone Joint Surg **86A,** 1541, 2004.
4. Muschler, G., Boehm, C., and Easley, K. Aspiration to obtain osteoblast progenitor cells from human bone marrow: the influence of aspiration volume. J Bone Joint Surg Am **79,** 1699, 1997.

5. Majors, A.K., Boehm, C.A., Nitto, H., Midura, R.J., and Muschler, G.F. Characterization of human bone marrow stromal cells with respect to osteoblastic differentiation. J Orthop Res **15,** 546, 1997.
6. Muschler, G., and Midura, R. Connective tissue progenitors: practical concepts for clinical applications. Clin Orthop **395,** 66, 2002.
7. Shinohara, K., Greenfield, S., Pan, H., Vasanji, A., Kumagai, K., Midura, R.J., Kiedrowski, M., Penn, M.S., and Muschler, G.F. Stromal cell-derived factor-1 and monocyte chemotactic protein-3 improve recruitment of osteogenic cells into sites of musculoskeletal repair. J Orthop Res **29,** 1064, 2011.
8. Boban, I., Barisic-Dujmovic, T., and Clark, S. Parabiosis model does not show presence of circulating osteoprogenitor cells. Genesis **48,** 171, 2010.
9. Hernigou, P., Poignard, A., Beaujean, F., and Rouard, H. Percutaneous autologous bone-marrow grafting for nonunions. Influence of the number and concentration of progenitor cells. J Bone Joint Surg Am **87,** 1430, 2005.
10. Muschler, G.F., Nitto, H., Matsukura, Y., Boehm, C., Valdevit, A., Kambic, H.E., Davros, W.J., Powell, K., and Easley, K. Spine fusion using cell matrix composites enriched in bone marrow-derived cells. Clin Orthop Relat Res **407,** 102, 2003.
11. Muschler, G.F., Matsukura, Y., Nitto, H., Boehm, C.A., Valdevit, A.D., Kambic, H.E., Davros, W.J., Easley, K.A., and Powell, K. Selective retention of bone marrow-derived cells to enhance spinal fusion. Clin Orthop **432,** 242, 2005.
12. Tiedeman, J.J., Connolly, J.F., Strates, B.S., and Lippiello L. Treatment of nonunion by percutaneous injection of bone marrow and demineralized bone matrix. An experimental study in dogs. Clin Orthop **268,** 294, 1991.
13. Connolly, J.F. Injectable bone marrow preparations to stimulate osteogenic repair. Clin Orthop **313,** 8, 1995.
14. Hernigou, P., Poignard, A., Manicom, O., Mathieu, G., and Rouard, H. The use of percutaneous autologous bone marrow transplantation in nonunion and avascular necrosis of bone. J Bone Joint Surg Br **87,** 896, 2005.
15. Simmons, P., and Torok-Storb, B. Identification of stromal cell precursors in human bone marrow by a novel monoclonal antibody. Blood **78,** 55, 1991.
16. Quirici, N., Soligo, D., Bossolasco, P., *et al.* Isolation of bone marrow mesenchymal stem cells by anti-nerve growth factor receptor antibodies. Exp Hematol **30,** 783, 2002.
17. Deschaseaux, F., and Chambord, P. Human marrow stromal cell precursors are alpha 1 integrin subunit-positive. J Cell Physiol **184,** 319, 2000.
18. Crisan, M., Yap, S., Casteilla, L., *et al.* A perivascular origin for mesenchymal stem cells in multiple human organs. Cell Stem Cell **3,** 301, 2008.
19. Boriet, N., Rapatel, C., Boisgard, S., *et al.* CD34+ CDw90(Thy-1)+subset collocated with mesenchymal progenitors in human normal bone marrow hematon units is enriched in colony forming unit megakaryocytes and long-term culture-initiating cells. Exp Hematol **31,** 1275, 2003.
20. Caralla, T., Boehm, C., Hascall, V., and Muschler, G. Hyaluronan as a novel marker for rapid selection of connective tissue progenitors. Ann Biomed Eng 2012 [Epub ahead of print]; DOI: 10.1007/s10439-012-0608-2.
21. Wang, A., and Hascall, V. Hyaluronan structures synthesized by rat mesangial cells in response to hyperglycemia induce monocyte binding. J Biol Chem **279,** 10279, 2004.
22. Takigami, H., Kumagai, K., Latson, L., Daisuke Togawa, D., Bauer, T., Powell, K., Butler, R.S., and Muschler, G.F. Bone formation following OP-1 implantation is improved by addition of autogenous bone marrow cells in a canine femur defect model. J Orthop Res **25,** 1333, 2007.
23. Muschler, G.F., Raut, V.P., Patterson, T.E., Wenke, J.C., and Hollinger, J.O. The design and use of animal models for translational research in bone tissue engineering and regenerative medicine. Tissue Eng Part B Rev **16,** 123, 2010.
24. Raut, V.P., Patterson, T.E., Wenke, J.C., Hollinger, J.O., and Muschler, G.F. Assessment of biomaterials: standardized *in vivo* testing. In: Guelcher, S.A., and Hollinger, J.O., eds. An Introduction to Biomaterials. Boca Raton, FL: CRC Press, 2010.
25. Villarruel, S., Boehm, C., Pennington, M., *et al.* The effect of oxygen tension on the *in vitro* assay of human osteoblastic connective tissue progenitor cells J Orthop Res **26,** 1390, 2008.
26. Powell, K., Nakamoto, C., Villarruel, S., *et al.* Quantitative image analysis of connective tissue progenitors. Anal Quant Cytol Histol **29,** 112, 2007.
27. Muir, J.M., Hirsh, J., Weitz, J.I., *et al.* A histomorphometric comparison of the effects of heparin and low-molecular weight heparin on cancellous bone in rats. Blood **89,** 3236 1997.
28. Nishiyama, M., Itoh, F., and Ujiie, A. Low-molecular-weight heparin (dalteparin) demonstrated a weaker effect on rat bone metabolism compared with heparin. Jpn J Pharmacol **74,** 59, 1997.
29. Kock, H.J., Werther, S., Uhlenkott, H., and Taeger, G. Influence of unfractionated and low-molecular-weight heparin on bone healing: an animal model. Unfallchirurg **105,** 791, 2002.
30. Erli, H., Melchert, M., and Rueger, M. The effect of low-dosed unfractioned and low-molecular-weight heparins on bone healing *in vivo*. Int J Orthop Surg 3, 2006. Available at www.ispub.com/ostia/index.php?xmlFilePath=journals/ijos/vol3n2/heparin.xml. DOI: 10.5580/1f1d.
31. Muschler, G.F., Huber, B., Ullman, T., Barth, R., Easley, K., Otis, J.O., and Lane, J.M. Evaluation of bone-grafting materials in a new canine segmental spinal fusion model. J Orthop Res **11,** 514, 1993.

Address correspondence to:
George F. Muschler, M.D.
Department of Biomedical Engineering (ND20)
Lerner Research Institute
Cleveland Clinic
9500 Euclid Ave.
Cleveland, OH 44195

E-mail: muschlg@ccf.org

Tonya Caralla, M.S.
Department of Biomedical Engineering (ND20)
Lerner Research Institute
Cleveland Clinic
9500 Euclid Ave.
Cleveland, OH 44195

E-mail: caralll@ccf.org

Received: November 2, 2011
Accepted: July 24, 2012
Online Publication Date: October 18, 2012